

11.8 Electrical Funnel: A Broadband Signal Combining Method

Ehsan Afshari¹, Harish Bhat^{1,2}, Xiaofeng Li^{1,3}, and Ali Hajimiri¹

¹California Institute of Technology, Pasadena, CA

²Columbia University, New York, NY

³Harvard University, Cambridge, MA

Recently, there has been growing interest in using silicon-based integrated circuits at high microwave and millimeter-wave frequencies. The high level of integration offered by silicon enables numerous new topologies and architectures for low-cost reliable SoC applications at microwave and millimeter-wave bands, such as broadband wireless access (e.g., WiMax), vehicular radars at 24GHz and 77GHz [1], short range communications at 24GHz and 60GHz, and ultra narrow pulse generation for UWB radar.

Power generation and amplification is one of the major challenges at millimeter-wave frequencies. This is particularly critical in silicon integrated circuits due to the limited gain, efficiency, and breakdown voltages for active devices and the lower quality factor of passive components caused by ohmic and substrate losses.

Efficient power combining is particularly useful in silicon where a large number of smaller power sources and/or amplifiers can generate large output power levels reliably. This would be most beneficial if the power combining function is merged with impedance transformation to allow individual transistors to drive more current with lower voltage swings to avoid breakdown [2]. Most traditional power combining methods use either resonant circuits and are, therefore, narrowband or employ broadband, yet lossy, resistive networks.

In this paper, we propose a general class of two-dimensional passive propagation media that can be used for power combining and impedance transformation among other things. These media take advantage of wave propagation in an inhomogeneous 2-D electrical lattice. Using this approach we show a power amplifier capable of generating 125mW at 85GHz in silicon.

A 1-D LC ladder can be generalized to a 2-D propagation medium by forming a lattice consisting of inductors (L) and capacitors (C). Figure 11.8.1 shows a square lattice. Generally, this lattice can be inhomogeneous where the L 's and C 's vary in space, and/or non-linear where they are current and/or voltage dependent. When the L 's and C 's do not change too abruptly, it is possible to define local propagation delay ($\propto \sqrt{LC}$) and local characteristic impedances ($\propto \sqrt{L/C}$) at each node. This allows us to define local impedance and velocity as functions of x and y , which can be engineered to achieve the desired propagation and reflection properties [3]. In this paper, we show one application of these 2-D lattices as a means for simultaneous power combining and impedance transformation.

One way these surfaces can be engineered is by keeping the propagation velocity constant vertically (constant LC product for a given y), while increasing the characteristic impedance at the top and bottom of the lattice at a faster rate as we move along the x axis to the right, as illustrated in Fig. 11.8.2. A planar wave propagating in the x direction from left to right gradually experiences higher impedances at the edges, creating a lower resistance path for the current in the middle; this *funnel*s more power to the center as the wave propagates to the right and simultaneously performs a gradual impedance transformation from the left to the right as illustrated by the simulated voltage and current waveforms of Fig. 11.8.3. By keeping the propagation velocity independent of y as we move along the x axis, we can maintain a plane wave keeping the lattice response frequency independent for the frequencies lower than its natural cut-off frequency [3]. We call

this an *electrical funnel* due to the way it combines and channels the power to the center at the output.

Multiple synchronous signal sources driving the low-impedance left-hand side of the funnel can generate a planar wave-front moving along the x axis. The output node is at the center of the right boundary. All of the nodes along the right boundary are terminated with resistors matched to the local impedances at the nodes. The up and down boundaries are kept open. The simulated efficiency of one implementation versus frequency is shown in Fig. 11.8.3 and demonstrates the broadband nature of the electrical funnel. Efficiency is defined as the ratio of the power at the output node to the sum of the powers of the inputs.

In practice, the characteristic impedance at the edges of the rectangular implementation keeps increasing as we move to the right; hence it is possible to discard the higher impedance parts of the mesh as we move to the right, effectively reducing it to a trapezoid. In a silicon process with multiple metals, we can use different metal layers as the ground plane at different points on the y axis. Our design uses four lower metal layers to form the variable-depth ground plane. This leads to different capacitance per unit length that can be used to control the local characteristic impedance across the combiner, as shown in Fig. 11.8.4. Since the variable-depth ground plane does not change the inductance, the propagation delay is not constant versus y , which results in a band-pass response. The output is matched to 50 Ω while each of the inputs is matched to around 15 Ω . The difference between this structure and a standard tapered transmission line is that this structure has a larger bandwidth (a 45% increase in this case) over a shorter distance (lower loss) due to the variable-depth ground plane. The new combiner is also smaller; 410 μm by 240 μm .

We used this combiner to design a power amplifier in a 0.13 μm SiGe BiCMOS process with a bipolar cutoff frequency of 200GHz. A die photo of the amplifier is shown in Fig. 11.8.5. In order to obtain a wideband response, we use degenerate cascode distributed amplifiers with emitter degeneration as input drivers. A non-degenerate cascode amplifying stage in this process has a maximum stable power gain of 15dB at 80GHz, as opposed to 7dB for a standard common-emitter amplifier. The cascode stages are emitter degenerated to improve bandwidth and avoid thermal runaway. Each of the four distributed amplifiers consists of eight cascode stages driving the output transmission line, which drive the inputs of the combiner.

The driver amplifiers have two power supplies of -2.5V and 0.8V and draw 750mA of current. Figure 11.8.6 shows the measured peak output power and gain of the amplifier versus frequency. The maximum output power was measured using two different signal sources: a backward wave oscillator (BWO) and a frequency multiplier. The overall small-signal gain is above 8dB at 85GHz where the peak power of 125mW is achieved. The lower measured maximum power in the multiplier measurement is due to its limited output power compared to a BWO and the lower amplifier gain above 86GHz. The output power and drain efficiency as a function of input power are shown in Fig. 11.8.7. At 85GHz, drain efficiency is more than 4% at the 3dB gain compression point. The amplifier has a 3dB power bandwidth of 24GHz (between 73GHz and 97GHz).

References:

- [1] U. R. Pfeiffer, et al., "A 77GHz SiGe Power Amplifier for Potential Applications in Automotive Radar Systems," *IEEE RFIC Symp.*, pp. 91-4, June, 2004.
- [2] I. Aoki, et al., "Distributed Active Transformer: A New Power Combining and Impedance Transformation Techniques," *IEEE T. Microwave Theory and Techniques*, pp. 316-332, Jan., 2002.
- [3] E. Afshari, et al., "Extremely Wideband Signal Shaping using one- and two Dimensional Non-uniform Nonlinear Transmission Lines," to appear in *Journal of Applied Physics*.

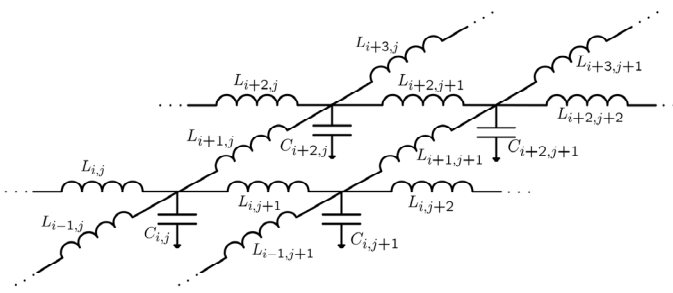


Figure 11.8.1: 2-D square electrical lattice.

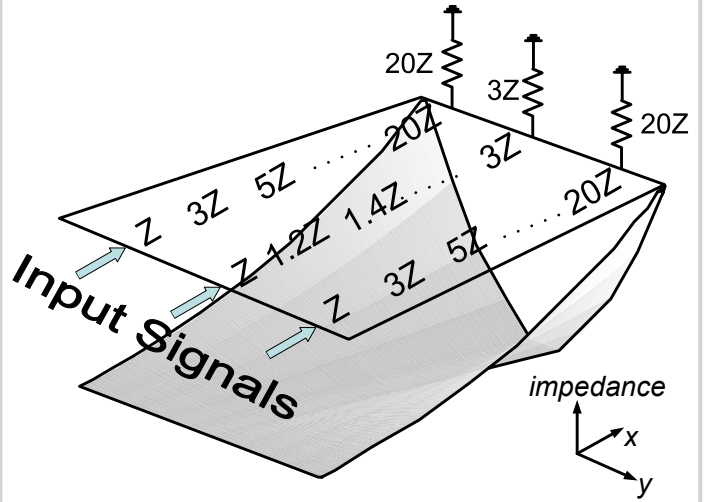


Figure 11.8.2: Illustration of the operation of a funnel.

11

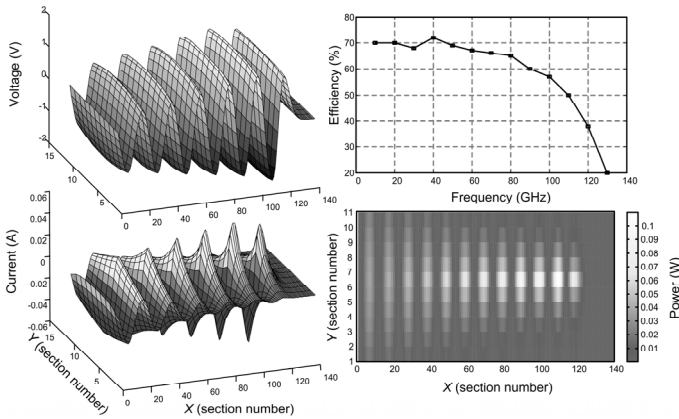


Figure 11.8.3: Simulation results for an ideal funnel with $30\text{pH} < L < 150\text{pH}$ and $30\text{fF} < C < 300\text{fF}$

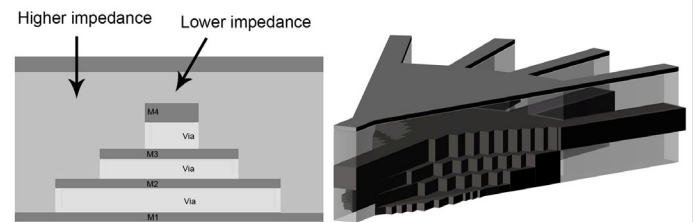


Figure 11.8.4: Combiner structure.

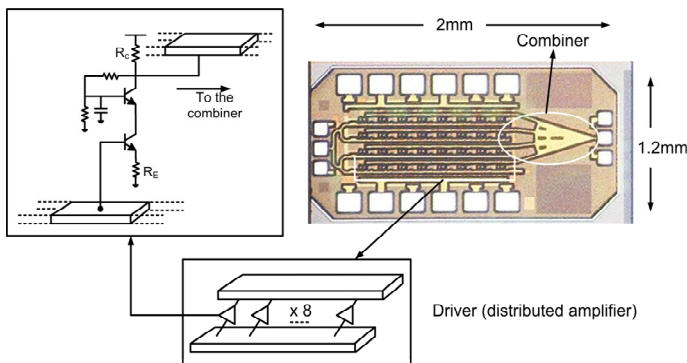


Figure 11.8.5: Die photo.

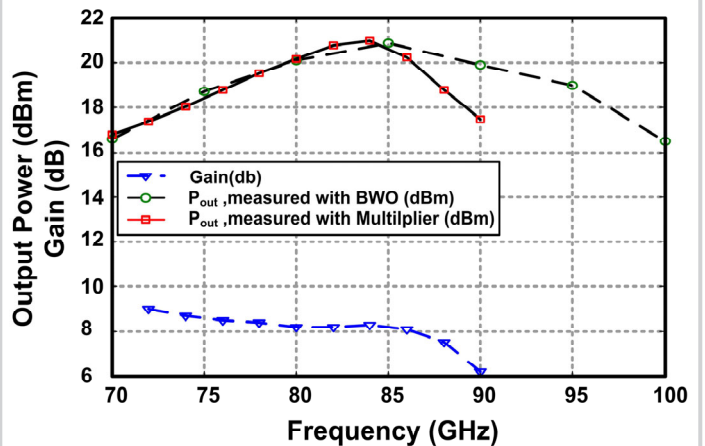


Figure 11.8.6: Measured saturated power and gain versus frequency.

Continued on Page

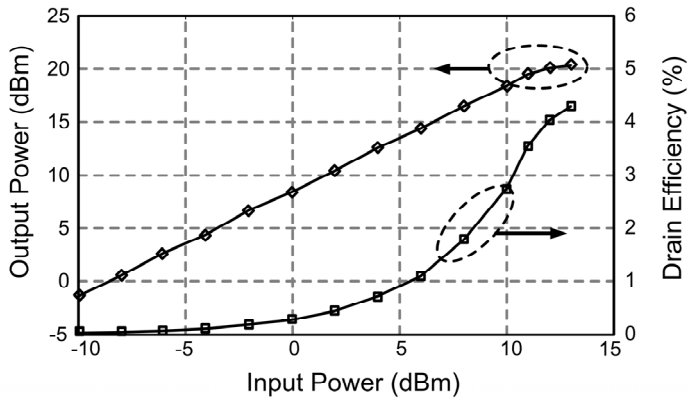


Figure 11.8.7: Measured large-signal parameters of the amplifier at 85GHz.